

Energy Management and Power Control of a Hybrid Active Wind Generator for Distributed Power Generation and Grid Integration

Tao Zhou and Bruno François, *Senior Member, IEEE*

Abstract—Classical wind energy conversion systems are usually passive generators. The generated power does not depend on the grid requirement but entirely on the fluctuant wind condition. A dc-coupled wind/hydrogen/supercapacitor hybrid power system is studied in this paper. The purpose of the control system is to coordinate these different sources, particularly their power exchange, in order to make controllable the generated power. As a result, an active wind generator can be built to provide some ancillary services to the grid. The control system should be adapted to integrate the power management strategies. Two power management strategies are presented and compared experimentally. We found that the “source-following” strategy has better performances on the grid power regulation than the “grid-following” strategy.

Index Terms—Distributed power, energy management, hybrid power system (HPS), power control, wind generator (WG).

I. INTRODUCTION

RENEWABLE energy sources (RES) and distributed generations (DGs) have attracted special attention all over the world in order to reach the following two goals:

- 1) the security of energy supply by reducing the dependence on imported fossil fuels;
- 2) the reduction of the emission of greenhouse gases (e.g., CO₂) from the burning of fossil fuels.

Other than their relatively low efficiency and high cost, the controllability of the electrical production is the main drawback of renewable energy generators, like wind turbines and photovoltaic panels, because of the uncontrollable meteorological conditions [1]. In consequence, their connection into the utility network can lead to grid instability or even failure if they are not properly controlled. Moreover, the standards for interconnecting these systems to the utility become more and more critical and require the DG systems to provide certain services, like frequency and voltage regulations of the local grid. Wind power is considered in this paper. Wind energy is the world's fastest growing energy source, expanding globally at a rate of 25%–35% annually over the last decade (Fig. 1) [2].

Manuscript received July 31, 2009; revised January 9, 2010 and February 26, 2010; accepted March 3, 2010. Date of publication March 29, 2010; date of current version December 10, 2010. This work was supported in part by the French National Research Agency (ANR) under ANR SuperEner Project and in part by the China Scholarship Council.

The authors are with the Université Lille Nord de France, 59000 Lille, France, and also with the Laboratoire d'Electrotechnique et d'Electronique de Puissance (L2EP), Ecole Centrale de Lille, 59651 Villeneuve d'Ascq, France (e-mail: taozhou123@hotmail.com; bruno.francois@ec-lille.fr).

Color versions of one or more of the figures in this paper are available online at <http://ieeexplore.ieee.org>.

Digital Object Identifier 10.1109/TIE.2010.2046580

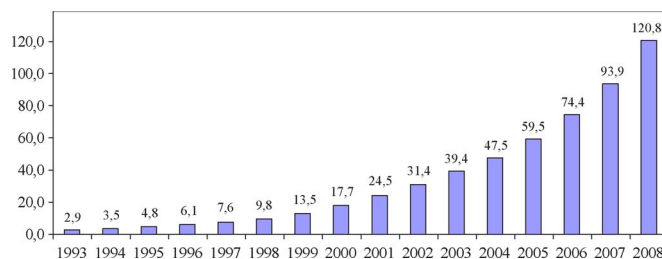


Fig. 1. Total wind power (in gigawatts) installed in the world since 1993 [2].

However, classical wind energy conversion systems work like passive generators. Because of the intermittent and fluctuant wind speed, they cannot offer any ancillary services to the electrical system in a microgrid application, where stable active- and reactive-power requirements should be attributed to the generators. As solutions, hybrid power systems (HPS) are proposed to overcome these problems with the following two innovative improvements.

- 1) *Energy storage systems* are used to compensate or absorb the difference between the generated wind power and the required grid power [3]–[6].
- 2) *Power management strategies* are implemented to control the power exchange among different sources and to provide some services to the grid [7]–[9].

Hydrogen technologies, combining fuel cells (FCs) and electrolyzers (ELs) with hydrogen tanks, are interesting for long-term energy storage because of the inherent high mass–energy density. In the case of wind energy surplus, the EL converts the excess energy into H₂ by electrochemical reaction. The produced H₂ can be stored in the hydrogen tank for future reutilization. In the case of wind energy deficit, the stored electrolytic H₂ can be reused to generate electricity by an FC to meet the energy demand of the grid. Thus, hydrogen, as an energy carrier, contributes directly to the reduction of dependence on imported fossil fuel [10], [11]. According to researchers, wind electrolysis is a very attractive candidate for an economically viable renewable hydrogen production system [12], [13]. However, FCs and ELs have low-dynamic performances, and fast-dynamic energy storage should be associated in order to overcome the fast fluctuations of wind power.

Recent progress in technology makes supercapacitors (SCs) the best candidates as fast dynamic energy storage devices, particularly for smoothing fluctuant energy production, like

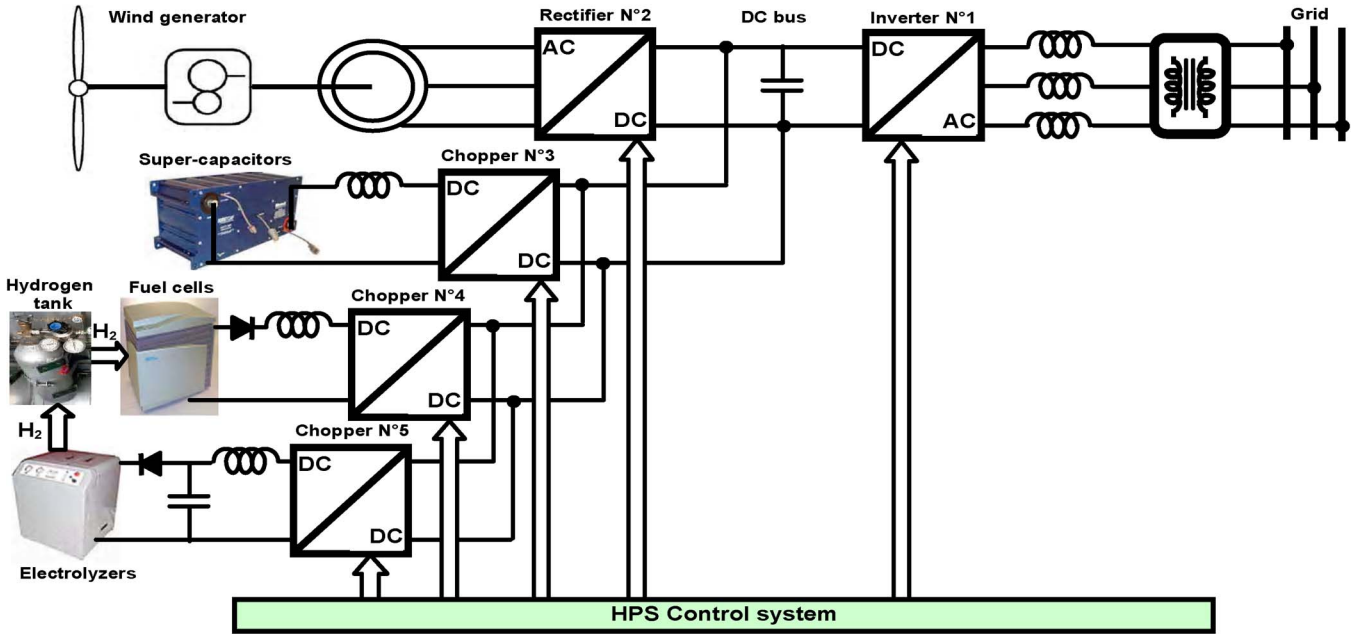


Fig. 2. Structure of the studied wind/hydrogen/SC HPS.

wind energy generators. Compared to batteries, SCs are capable of very fast charges and discharges and can achieve a very large number of cycles without degradation, even at 100% depth of discharge without “memory effect.” Globally, SCs have a better round-trip efficiency than batteries. With high dynamics and good efficiency, flywheel systems are also suitable for fast-dynamic energy storage [14], [15]. However, this mechanical system is currently hampered by the danger of “explosive” shattering of the massive wheel due to overload (tensile strength because of high weight and high velocity). SCs are less sensitive in operating temperature than batteries and have no mechanical security problems.

In order to benefit from various technology advantages, we have developed a wind generator (WG), including three kinds of sources: 1) a RES: WG; 2) a fast-dynamic storage: SCs; and 3) a long-term storage: FC, EL, and H₂ tank. The control of internal powers and energy management strategies should be implemented in the control system for satisfying the grid requirements while maximizing the benefit of RESs and optimizing the operation of each storage unit [16]. The purpose of this paper is to present the proposed power management strategies of the studied HPS in order to control the dc-bus voltage and to respect the grid according to the microgrid power requirements. These requirements are formulated as real- and reactive-power references, which are calculated by a centralized secondary control center in order to coordinate power dispatch of several plants in a control area. This area corresponds to a microgrid and is limited due to the high level of reliability and speed required for communications and data transfer [17]–[20].

In Sections II and III, the studied HPS structure is presented. The structure of the control system is adapted in order to integrate power management strategies. Two power management strategies are presented in Section IV. The experimental tests are presented to compare their performances in Section V, and conclusions are given in Section VI.

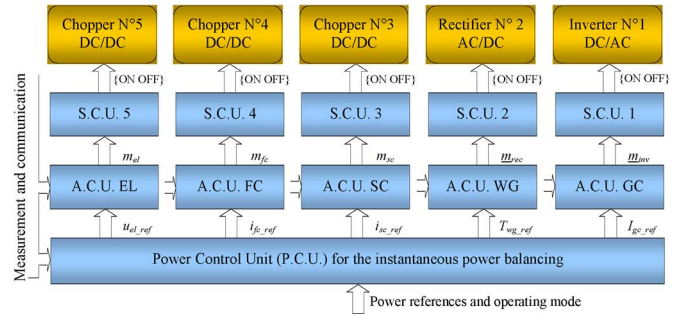


Fig. 3. Hierarchical control structure of the HPS.

II. HPS AND CONTROL SYSTEM

A. Structure of HPS

In this paper, we use a dc-coupled structure in order to decouple the grid voltages and frequencies from other sources. All sources are connected to a main dc bus before being connected to the grid through a main inverter (Fig. 2) [21]–[23]. Each source is electrically connected with a power-electronic converter in order to get possibilities for power control actions. Moreover, this HPS structure and its global control system can also be used for other combinations of sources.

B. Structure of Control System

Power converters introduce some control inputs for power conversion. In this case, the structure of the control system can be divided into different levels (Fig. 3) [7].

The *switching control unit (SCU)* is designed for each power converter. In an SCU, the drivers with optocouplers generate the transistor’s ON/OFF signals from the ideal states of the switching function $\{0, 1\}$, and the modulation technique (e.g.,

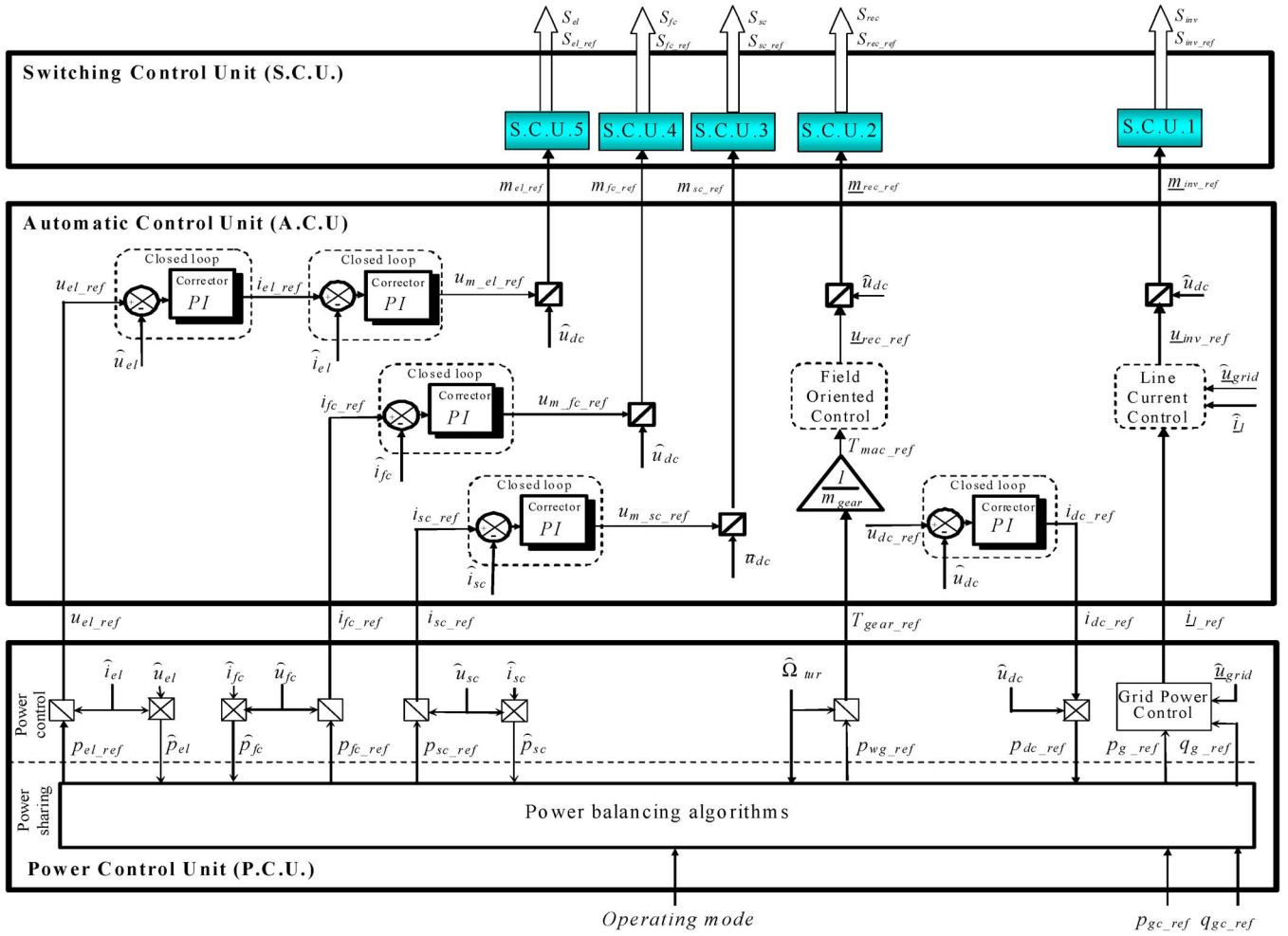


Fig. 4. Modeling and control of the HPS by the Energetic Macroscopic Representation.

pulsewidth modulation) determines the switching functions from the modulation functions (m).

The **automatic control unit (ACU)** is designed for each energy source and its power conversion system. In an ACU, the control algorithms calculate the modulation functions (m) for each power converter through the regulation of some physical quantities according to their reference values.

The **power control unit (PCU)** is designed to perform the instantaneous power balancing of the entire HPS in order to satisfy the grid requirements. These requirements are real- and reactive-power references, which are obtained from the secondary control center and from references of droop controllers [24], [25]. In a PCU, some power-balancing algorithms are implemented to coordinate the power flows of different energy sources. The different power-balancing algorithms correspond to a number of possible operating modes of the HPS and can be gathered.

The purpose of this paper is to present the power-balancing strategies in the PCU. In order to focus on the power-balancing strategies of the HPS, the control schemes of the power conversion systems through different power converters will not be detailed in this paper. However, some explanations of the ACUs are given in the following paragraphs in order to make the controllable variables of the power conversion systems appear.

C. ACU

The control schemes in the ACUs are shown in Fig. 4 with block diagrams.

- 1) The **EL power conversion system** is controlled by setting the terminal voltage (u_{el}) equal to a prescribed reference (u_{el_ref}) through the dc chopper N°5. The EL stack is considered as an equivalent current source (i_{el}).
- 2) The **FC power conversion system** is controlled with a reference of the FC current (i_{fc_ref}) through the dc chopper N°4. The FC stack is considered as an equivalent voltage source (u_{fc}).
- 3) The **SC power conversion system** is controlled with a current reference (i_{sc_ref}) through the dc chopper N°3. The SC bank is considered as an equivalent voltage source (u_{sc}).
- 4) The **wind energy conversion system** is controlled with a reference of the gear torque (T_{gear_ref}) by the three-phase rectifier N°2.
- 5) The **grid connection system** consists of a dc-bus capacitor and a grid power conversion system. The grid power conversion system is controlled with line-current references (i_{l_ref}) by the three-phase inverter N°1, because the grid transformer is considered as an equivalent voltage source (u_{grid}).

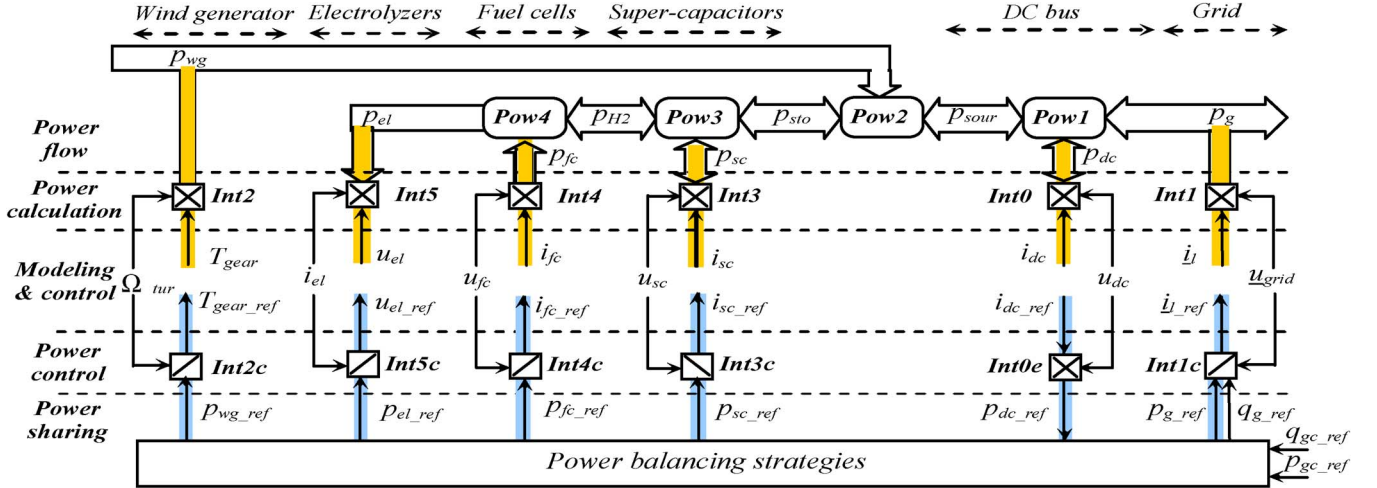


Fig. 5. Multilevel representation of the power modeling and control of the HPS.

The dc-bus voltage is described as

$$C_{dc} \frac{du_{dc}}{dt} = i_{dc}. \quad (1)$$

In order to control the dc-bus voltage, a voltage controller must be used. The output of the voltage controller is a current reference i_{dc_ref} (Fig. 4).

III. PCU

A. Layout of PCU

The power modeling of the HPS can be divided into two levels: the **power calculation level** and the **power flow level** (Fig. 5). Thus, the PCU is also divided into two levels: the **power control level** and the **power sharing level**.

The PCU enables one to calculate references for the ACU from power references. The power sharing level coordinates the power flow exchanges among the different energy sources with different power-balancing strategies. They are presented here in detail with the help of the Multilevel Representation (Fig. 5), which was developed by Peng Li in 2008 [26].

B. Power Control Level

The power exchanges with various sources are controlled only via the related five references (u_{el_ref} , i_{fc_ref} , i_{sc_ref} , T_{gear_ref} , and \dot{i}_l_ref in Fig. 5). Therefore, the expressions of the powers should be deduced in order to obtain these power references (Table I). Only the sources' powers and the exchanged power with the dc-bus capacitor are taken into account here.

For the energy storage systems, the powers are calculated by multiplying the measured currents and the measured voltages (**Int3**, **Int4**, and **Int5** in Table I). The references of the controllable variables are obtained by dividing the power reference with the measured current or the measured voltages (**Int3c**, **Int4c**, and **Int5c** in Table I).

For the wind energy conversion system, a maximal-power-point-tracking (MPPT) strategy is used to extract the maximum power of the available wind energy according to a nonlinear characteristic in function of the speed. It receives the measured

TABLE I
SUMMARY OF EQUATIONS FOR POWER CALCULATION

	Power calculation	Power control
DC	Int0 : $p_{dc} = u_{dc} i_{dc}$	Int0e : $p_{dc_ref} = u_{dc} i_{dc_ref}$
GC	Int1 : $\begin{cases} p_g = u_{13} i_1 + u_{23} i_2 \\ q_g = \sqrt{3}(u_{13} i_1 - u_{23} i_2) \end{cases}$	Int1c : $\begin{cases} i_{i1_ref} = \frac{(2u_{13} - u_{23})p_{g_ref} + \sqrt{3}u_{23}q_{g_ref}}{2u_{13}^2 - 2u_{13}u_{23} + 2u_{23}^2} \\ i_{i2_ref} = \frac{(2u_{23} - u_{13})p_{g_ref} - \sqrt{3}u_{13}q_{g_ref}}{2u_{13}^2 - 2u_{13}u_{23} + 2u_{23}^2} \end{cases}$
WG	Int2 : $p_{wg} = \Omega_{gear} T_{gear}$	Int2c : $T_{gear_ref} = p_{wg_ref} / \Omega_{gear}$
SC	Int3 : $p_{sc} = u_{sc} i_{sc}$	Int3c : $i_{sc_ref} = p_{sc_ref} / u_{sc}$
FC	Int4 : $p_{fc} = i_{fc} u_{fc}$	Int4c : $i_{fc_ref} = p_{fc_ref} / u_{fc}$
EL	Int5 : $p_{el} = i_{el} u_{el}$	Int5c : $u_{el_ref} = p_{fc_ref} / i_{fc}$

rotational speed (Ω_{tur}) and sets a desired power reference (p_{wg_ref}) (**Int2** and **Int2c** in Table I).

The output of the dc-bus voltage control loop is the current reference (i_{dc_ref}) of the dc-bus capacitor, and its product with the measured dc-bus voltage gives the power reference (p_{dc_ref}) for the dc-bus voltage regulation (**Int0e**). The powers, which are exchanged with the grid, can be calculated with the "two-wattmeter" method (**Int1** and **Int1c** in Table I).

In order to focus on the power exchanges with the different sources around the dc bus, the instantaneously exchanged power with the choke, the losses in the filters, and the losses in the power converters are neglected.

C. Power Sharing Level

The power sharing level is used to implement the power-balancing strategies in order to coordinate the various sources in the HPS (Fig. 5). It plays a very important role in the control system, because the power exchanges lead directly to the stability of the HPS and impact the dc-bus voltage (u_{dc})

$$\frac{dE_{dc}}{dt} = C_{dc} u_{dc} \frac{du_{dc}}{dt} = p_{dc} = p_{wg} + p_{sc} + p_{fc} - p_{el} - p_g \quad (2)$$

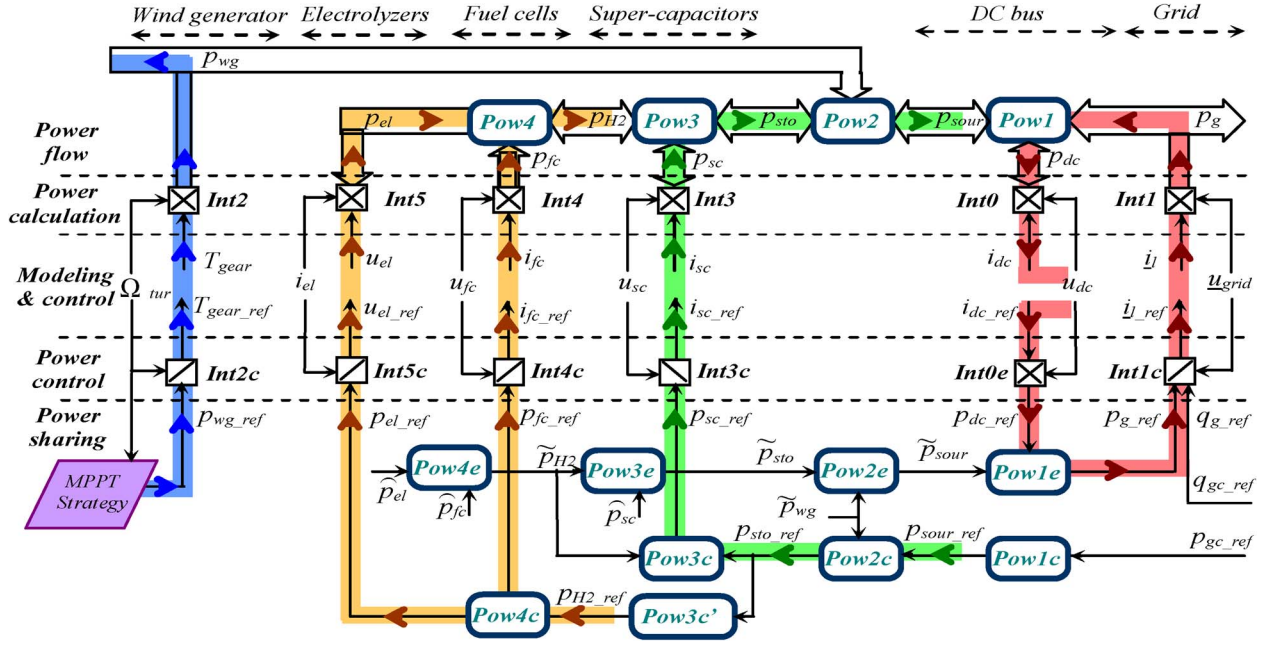


Fig. 6. Multilevel representation of the grid-following strategy.

with

E_{dc} stored energy in the dc-bus capacitor;
 p_{dc} resulted power into the dc-bus capacitor;
 p_{wg} generated power from the WG;
 p_{fc} generated power from the FC;
 p_{sc} exchanged power with the SC;
 p_{el} consumed power by the EL;
 p_g delivered power into the grid from the dc bus.

According to the power exchange, the power flows inside this HPS are modeled with four equations

$$\mathbf{Pow1} : p_g = p_{sour} - p_{dc} \quad (3)$$

$$\mathbf{Pow2} : p_{sour} = p_{sto} + p_{wg} \quad (4)$$

$$\mathbf{Pow3} : p_{sto} = p_{H2} + p_{sc} \quad (5)$$

$$\mathbf{Pow4} : p_{H2} = p_{fc} - p_{el} \quad (6)$$

with

p_{sour} “source” total power arriving at the dc bus;
 p_{sto} “storage” total power arriving at the dc bus;
 p_{H2} “hydrogen” total power arriving at the dc bus.

In this wind/hydrogen/SC HPS, five power-electronic converters are used to regulate the power transfer with each source. According to a chosen power flow, the following two power-balancing strategies can be implemented.

- 1) The **grid-following strategy** uses the line-current loop to regulate the dc-bus voltage.
- 2) The **source-following strategy** uses the line-current loop to control the grid active power, and the dc-bus voltage is regulated with the WG and storage units.

IV. POWER-BALANCING STRATEGIES

A. Grid-Following Strategy

With the grid-following strategy, the dc-bus voltage is regulated by adjusting the exchanged power with the grid, while the WG works in MPPT strategies [27]. In Fig. 6, the dc-bus voltage control is shown by a closed loop ($p_{dc_ref} \rightarrow p_{g_ref} \rightarrow p_g \rightarrow p_{dc}$). Thus, the required power for the dc-bus voltage regulation (p_{dc_ref}) is used to estimate the grid power reference (p_{g_ref})

$$\mathbf{Pow1e} : p_{g_ref} = \tilde{p}_{sour} - \tilde{p}_{dc_ref}. \quad (7)$$

The source total power (p_{sour}) is a disturbance and should also be taken into account with the estimated wind power and the sensed total storage power

$$\mathbf{Pow2e} : \tilde{p}_{sour} = \tilde{p}_{wg} + \tilde{p}_{sto}. \quad (8)$$

The energy storage systems help the wind energy conversion system satisfy the power references, which are asked by the microgrid operator

$$\mathbf{Pow3e} : \tilde{p}_{sto} = \hat{p}_{sc} + \hat{p}_{H2} \quad (9)$$

$$\mathbf{Pow4e} : \tilde{p}_{H2} = \hat{p}_{fc} - \hat{p}_{el}. \quad (10)$$

In steady state, the dc-bus voltage is regulated, and the averaged power exchange with the dc-bus capacitor can be considered as zero in (3). Hence, in steady state, the grid power (p_g) is equal to the total power from the sources (p_{sour}). If the microgrid system operator sets a power requirement (p_{gc_ref}), it must be equal to the sources' power reference (p_{sour_ref}), as shown in Fig. 6

$$\mathbf{Pow1c} : p_{sour_ref} = p_{g_ref} = p_{gc_ref}. \quad (11)$$

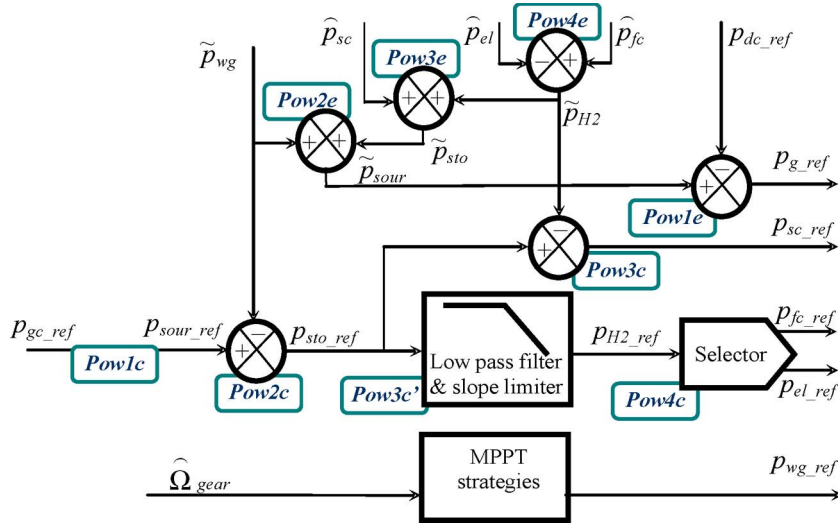


Fig. 7. Block diagram of the grid-following strategy.

In order to help the wind energy conversion system respect the active-power requirement, the energy storage systems should be coordinated to supply or absorb the difference between this power requirement (p_{gc_ref}) and the fluctuant wind power (p_{wg}), as shown in Fig. 6

$$\mathbf{Pow2c} : p_{sto_ref} = p_{sour_ref} = \tilde{p}_{wg}. \quad (12)$$

Among the energy storage systems, the FCs and the ELs are the main energy exchangers because a large quantity of hydrogen can be stored for enough energy availability. For efficiency reasons, the FC and the EL should not work at the same time. The activation of the FC or the activation of the EL depends on the sign of the reference (p_{H2_ref}). Thus, a selector assigns the power reference (p_{H2_ref}) to the FC (p_{fc_ref}) or to the EL (p_{el_ref}) according to the sign of p_{H2_ref} (Fig. 6)

$\mathbf{Pow4c} :$

$$\begin{cases} \text{if: } p_{H2_ref} > \varepsilon, & p_{fc_ref} = p_{H2_ref}; p_{el_ref} = 0 \\ \text{if: } |p_{H2_ref}| \leq \varepsilon, & p_{fc_ref} = 0; p_{el_ref} = 0 \\ \text{if: } p_{H2_ref} < -\varepsilon, & p_{fc_ref} = 0; p_{el_ref} = |p_{H2_ref}|. \end{cases} \quad (13)$$

However, the power reference (p_{sto_ref}) is a fast-varying quantity due to the fluctuant wind power (p_{wg}) and the varying grid power (p_g). In order to avoid the fast-chattering problem when it is close to zero, it should be slowed down. Moreover, the FCs and the ELs have relatively slow power dynamics, and fast-varying power references are not welcome for their operating lifetime. Therefore, a low-pass filter (LPF) with a slope limiter should be added (Fig. 6)

$$\mathbf{Pow3c}' : p_{H2_ref} = \frac{1}{1 + \tau s} (p_{sto_ref}) \quad (14)$$

where τ is the time constant of the LPF and should be set large enough by taking into account the power dynamics of the FCs and the ELs, as well as the size of the SCs.

The SCs are not made for a long-term energy backup unit because they have limited energy storage capacities due to

their low energy density. However, they have very fast power dynamics and can supply fast-varying powers and power peaks. They can be used as an auxiliary power system of the FCs and ELs to fill the power gaps during their transients

$$\mathbf{Pow3c} : p_{sc_ref} = p_{sto_ref} - \hat{p}_{H2} = p_{sto_ref} - \hat{p}_{fc} + \hat{p}_{el}. \quad (15)$$

The block diagram of the grid-following strategy for the active WG is shown in Fig. 7.

B. Source-Following Strategy

The total power (p_{sour}) from the energy storage and the WG can also be used to provide the necessary dc power (p_{dc}) for the dc-bus voltage regulation (Fig. 8) [27]. In this case, the necessary total power reference (p_{sour_ref}) must be calculated by taking into account the required power for the dc-bus voltage regulation (p_{dc_ref}) and the measured grid power (p_g) as disturbance input by using the inverse equation of $\mathbf{Pow1}$ (Fig. 8)

$$\mathbf{Pow1c} : p_{sour_ref} = p_{dc_ref} + \hat{p}_g. \quad (16)$$

Then, the total power reference of the storage systems is deduced by taking into account the fluctuant wind power with the inverse equation of $\mathbf{Pow2}$ (Fig. 8)

$$\mathbf{Pow2c} : p_{sto_ref} = p_{sour_ref} - \tilde{p}_{wg}. \quad (17)$$

This power reference is shared among the FCs, the ELs, and the SCs in the same way as explained earlier ($\mathbf{Pow2c}$, $\mathbf{Pow3c}$, $\mathbf{Pow4c}$, and $\mathbf{Pow3c}'$).

In addition, now, the grid power reference (p_{g_ref}) is free to be used for the grid power control. The microgrid system operator can directly set the power requirements (p_{gc_ref} and q_{gc_ref}) for the grid connection system ($p_{g_ref} = p_{gc_ref}$). Therefore, the HPS can directly supply the required powers for providing the ancillary services to the microgrid, like the regulations of the grid voltage and frequency.

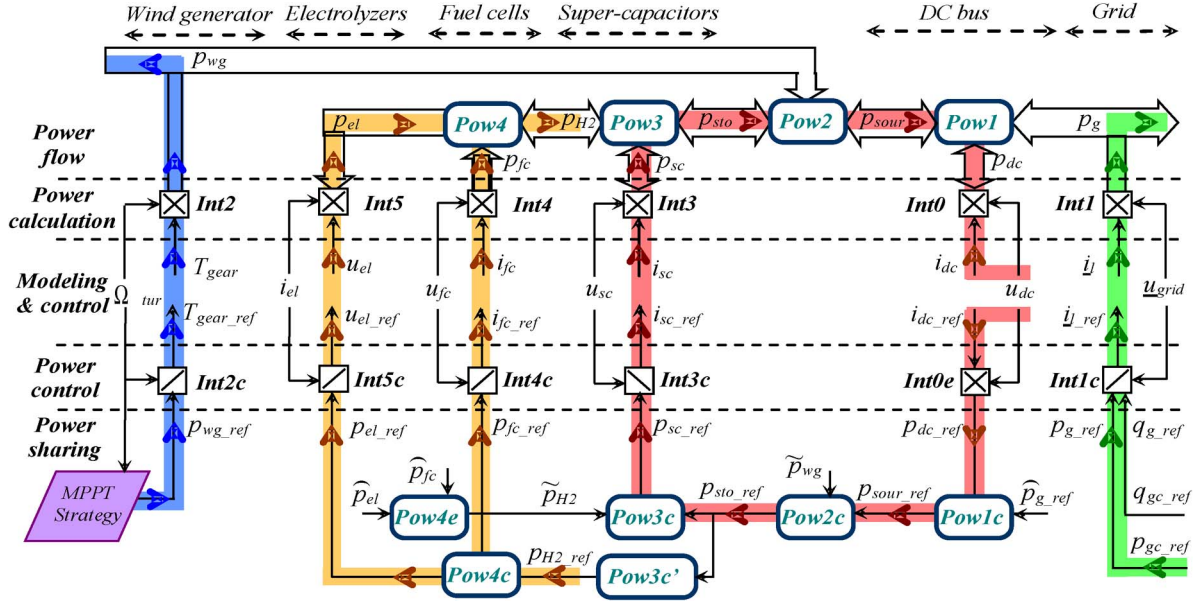


Fig. 8. Multilevel representation of the source-following strategy.

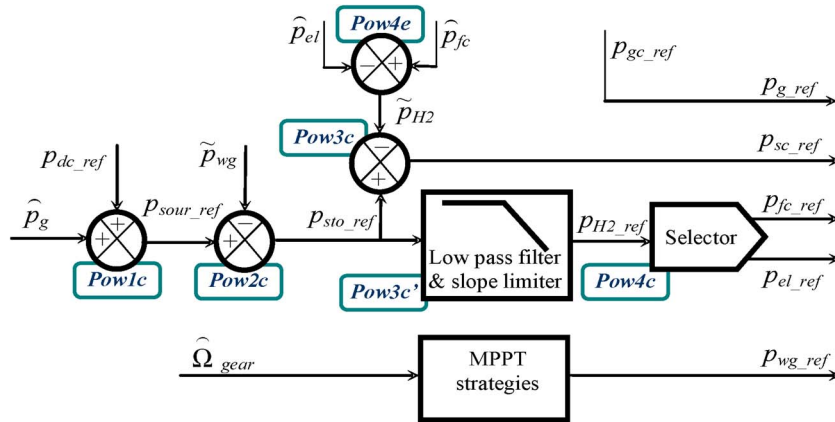


Fig. 9. Block diagram of the source-following strategy.

The block diagram of the grid-following strategy for the active WG is shown in Fig. 9.

V. EXPERIMENTAL TESTS

A. Experimental Platform Assessment

An experimental platform of the HPS has been built to test the different power-balancing strategies. Hardware-In-the-Loop (HIL) emulations of a part of a power system enable a fast experimental validation test before implementation with the real process. Some parts of the emulator process are simulated in real time in a controller board and are then interfaced in hardware with the real devices. Such a HIL simulation has been intensively used and enables one to check the availability and reliability of the hybrid active WG (storage component sizing, power-electronic interface, and operation control).

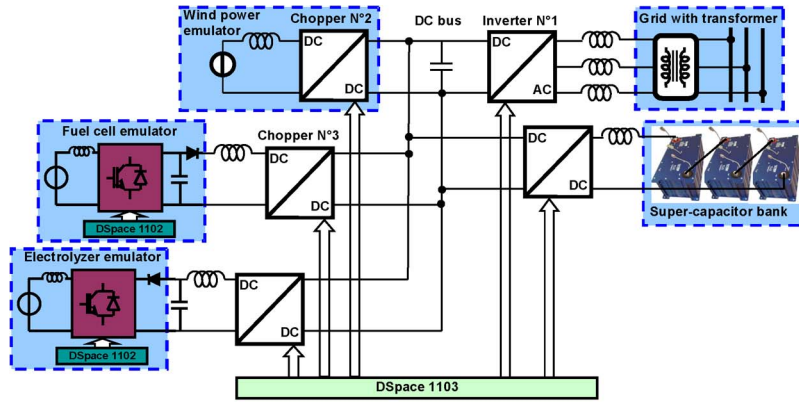
The FC and EL emulators are used to provide the same electrical behavior as the real FC stack and the EL stack [28]. Models of the FCs and the EL have been previously validated through comparisons with obtained experimental results and simulated results from models. They are implemented in a

digital control board (DSPACE 1102) and calculated voltages and currents are generated by using power-electronic converters. Three “Boostcap SC” modules (160 F and 48 V) are connected in series (Table II). Therefore, the equivalent capacitor of the SC bank is about 53 F, and the maximal voltage is about 144 V. All sources are connected to the dc bus through different power converters (Fig. 10). The dc bus is connected to the grid through a three-phase inverter, three line filters, and a grid transformer. Moreover, the HPS is controlled by a digital control board (DSPACE 1103).

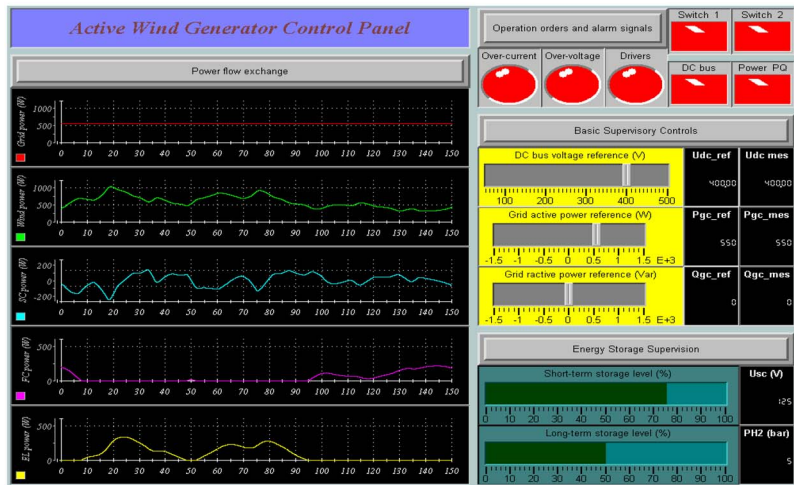
The wind power emulator is used to provide the predefined reduced wind power profile p_{wg} (1.2 kW). The sizing of the FC and EL stacks is adapted by using the modeling parameters of Table II in the HIL simulation in order to be interfaced in the experimental test bench. Two power-balancing strategies are

TABLE II
IMPLEMENTATION OF THE FC AND EL EMULATORS

	Number of cells	Active surface	Nominal power	Time constant
Fuel cells	156	25 cm ²	1 kW	5 s
Electrolyzers	70	15 cm ²	1 kW	5 s



(a)



(b)

Fig. 10. Implementation of the experimental test bench. (a) System structure. (b) Human-machine interface.

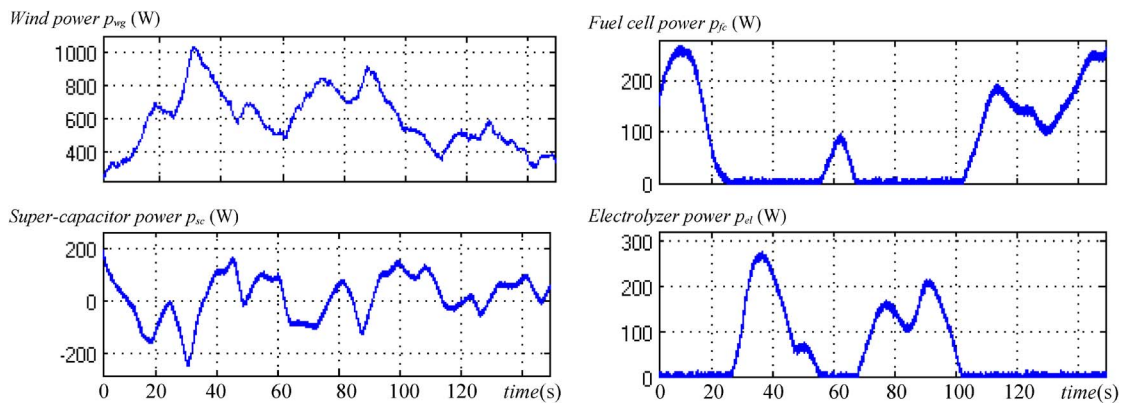


Fig. 11. Power profiles of the different sources.

tested and compared, respectively. With this experimental test bench, it is possible to apply our proposed hierarchical control system for the active generator and to test it with the developed power-balancing strategies.

B. Power Profile of Different Sources

Two tests are performed experimentally for both strategies, respectively. The same fluctuant wind power profile is used during 150 s (Fig. 11). The active-power requirement from

the microgrid is assumed to be $p_{gc_ref} = 600W$. Similar power profiles are obtained for the energy storage systems (Fig. 11). When the generated wind power is more than 600 W, the EL is activated to absorb the power difference, but when the generated wind power is less than 600 W, the FC is activated to compensate the power difference. Since the power dynamics of the FCs and the EL are limited by an LPF with a 5-s time constant, they are not able to filter the fast fluctuations of the wind power. Therefore, the SCs supply or absorb the power difference.

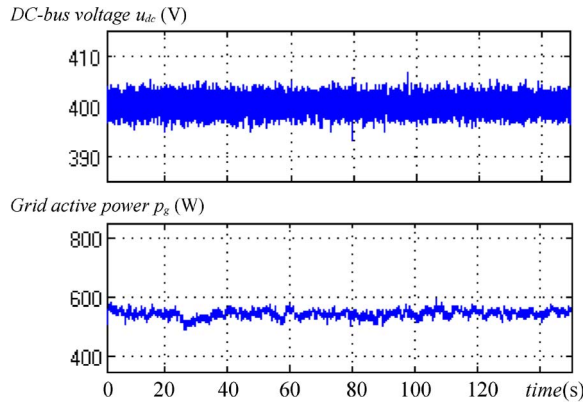


Fig. 12. Grid-following strategy test results.

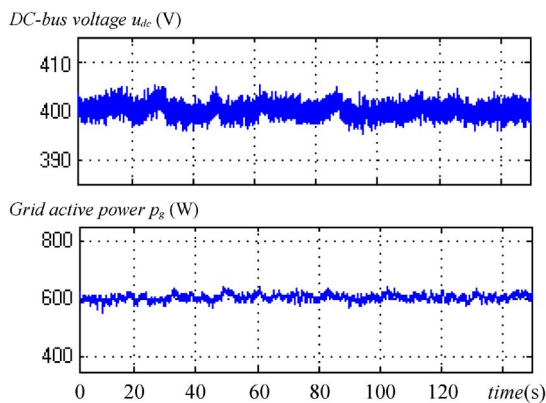


Fig. 13. Source-following strategy test results.

C. Grid Following Strategy

In the grid-following strategy, the dc-bus voltage is well regulated around 400 V by the grid power conversion system (Fig. 12). The energy storage systems help the WG supply the microgrid power requirement ($p_{\text{sour}} = p_{\text{gc_ref}} = 600$ W). Because of the different power losses in the filters and power converters, the grid active power is slightly less than the microgrid's requirement ($p_g < p_{\text{gc_ref}} = 600$ W).

D. Source-Following Strategy

In the source-following strategy, the energy storage systems are controlled to supply or absorb the necessary powers in order to maintain the dc-bus voltage (around 400 V) against the fluctuant wind power (Fig. 13). The grid active power is also regulated and is equal to the microgrid's requirement, because the line-current control loop regulates directly the grid powers ($p_g = p_{\text{gc_ref}} = 600$ W). Therefore, the source-following strategy has better performances on the grid power regulation than the grid-following strategy, and it can provide ancillary services according to the microgrid's requirements.

E. Comparison and Discussion

Thanks to the help of energy storage systems, the dc-bus voltage and the grid powers can be well regulated with both

power-balancing strategies, while the WG extracts the maximum available wind power.

By comparing the two power-balancing strategies with their experimental test results (Figs. 12 and 13), we see that the grid active power is better regulated in the “grid-following” strategy than in the “source-following” strategy. In the grid-following strategy, the grid power varies continuously because the line-current control loop regulates the dc-bus voltage and the grid power is adjusted all the time. In the source-following strategy, the dc-bus voltage is regulated by the SCs, and the grid power can be directly used to supply the same power as required by the microgrid system operator. Thus, if the active generator is required to provide the necessary powers to participate in the microgrid management, the source-following strategy is preferred for more precisely controlling the grid powers.

VI. CONCLUSION

In this paper, a dc-coupled HPS has been studied with the three kinds of energy sources: 1) a WG as a renewable energy generation system; 2) SCs as a fast-dynamic energy storage system; and 3) FCs with ELs and hydrogen tank as a long-term energy storage system. The structure of the control system is divided into three levels: 1) SCU; 2) ACU; and 3) PCU. Two power-balancing strategies have been presented and compared for the PCU: the grid-following strategy and the source-following strategy. For both of them, the dc-bus voltage and the grid power can be well regulated. The experimental tests have shown that the source-following strategy has better performance on the grid power regulation than the grid-following strategy.

REFERENCES

- [1] W. Li, G. Joos, and J. Belanger, “Real-time simulation of a wind turbine generator coupled with a battery supercapacitor energy storage system,” *IEEE Trans. Ind. Electron.*, vol. 57, no. 4, pp. 1137–1145, Apr. 2010.
- [2] [Online]. Available: <http://www.eurobserv-er.org/>
- [3] G. Delille and B. Francois, “A review of some technical and economic features of energy storage technologies for distribution systems integration,” *Ecol. Eng. Environ. Prot.*, vol. 1, pp. 40–49, 2009.
- [4] C. Abbey and G. Joos, “Supercapacitor energy storage for wind energy applications,” *IEEE Trans. Ind. Electron.*, vol. 43, no. 3, pp. 769–776, May 2007.
- [5] G. Taljan, M. Fowler, C. Cañizares, and G. Verbič, “Hydrogen storage for mixed wind-nuclear power plants in the context of a Hydrogen Economy,” *Hydrogen Energy*, vol. 33, no. 17, pp. 4463–4475, Sep. 2008.
- [6] M. Little, M. Thomson, and D. Infield, “Electrical integration of renewable energy into stand-alone power supplies incorporating hydrogen storage,” *Hydrogen Energy*, vol. 32, no. 10, pp. 1582–1588, Jul. 2007.
- [7] T. Zhou, D. Lu, H. Fakhm, and B. Francois, “Power flow control in different time scales for a wind/hydrogen/super-capacitors based active hybrid power system,” in *Proc. EPE-PEMC*, Poznan, Poland, Sep. 2008, pp. 2205–2210.
- [8] F. Baalbergen, P. Bauer, and J. A. Ferreira, “Energy storage and power management for typical 4Q-load,” *IEEE Trans. Ind. Electron.*, vol. 56, no. 5, pp. 1485–1498, May 2009.
- [9] D. Ipsakis, S. Voutetakis, P. Seferlis, F. Stergiopoulos, and C. Elmasides, “Power management strategies for a stand-alone power system using renewable energy sources and hydrogen storage,” *Hydro. Energy*, vol. 4, no. 16, pp. 7081–7095, Aug. 2009.
- [10] U.S. Department of Energy, Energy Efficiency and Renewable Energy, Wind & Hydropower Technologies Program, Wind Energy Research Area. [Online]. Available: <http://www.eere.energy.gov>
- [11] M. Lebbal, T. Zhou, B. Francois, and S. Lecoeuche, “Dynamically electrical modelling of electrolyzer and hydrogen production regulation,” in *Proc. Int. Hydrogen Energy Congr. Exhib.*, Istanbul, Turkey, Jul. 2007.

- [12] R. M. Dell and D. A. J. Rand, "Energy storage—A key technology for global energy sustainability," *Power Sources*, vol. 100, no. 1/2, pp. 2–17, Nov. 2001.
- [13] B. D. Shakyaa, L. Ayea, and P. Musgraveb, "Technical feasibility and financial analysis of hybrid wind–photovoltaic system with hydrogen storage for Cooma," *Hydro. Energy*, vol. 30, no. 1, pp. 9–20, Jan. 2005.
- [14] O. Gabriel, C. Saudemont, B. Robyns, and M. M. Radulescu, "Control and performance evaluation of a flywheel energy-storage system associated to a variable-speed wind generator," *IEEE Trans. Ind. Electron.*, vol. 53, no. 4, pp. 1074–1085, Aug. 2006.
- [15] R. Cardenas *et al.*, "Control strategies for power smoothing using a flywheel driven by a sensorless vector-controlled induction machine operating in a wide speed range," *IEEE Trans. Ind. Electron.*, vol. 51, no. 3, pp. 603–614, Jun. 2004.
- [16] P. Li, P. Degobert, B. Robyns, and B. Francois, "Participation in the frequency regulation control of a resilient microgrid for a distribution network," *Int. J. Integr. Energy Syst.*, vol. 1, no. 1, Jan. 2009.
- [17] J. M. Guerrero, J. C. Vasquez, J. Matas, M. Castilla, and L. G. de Vicuna, "Control strategy for flexible microgrid based on parallel line-interactive UPS systems," *IEEE Trans. Ind. Electron.*, vol. 56, no. 3, pp. 726–736, Feb. 2009.
- [18] C. Sudipta, D. W. Manoja, and M. G. Simoes, "Distributed intelligent energy management system for a single-phase high-frequency AC microgrid," *IEEE Trans. Ind. Electron.*, vol. 54, no. 1, pp. 97–109, Feb. 2007.
- [19] D. M. Vilathgamuwa, C. L. Poh, and Y. Li, "Protection of microgrids during utility voltage sags," *IEEE Trans. Ind. Electron.*, vol. 53, no. 5, pp. 1427–1436, Oct. 2006.
- [20] M. Prodanovic and T. C. Green, "High-quality power generation through distributed control of a power park microgrid," *IEEE Trans. Ind. Electron.*, vol. 53, no. 5, pp. 1427–1436, Oct. 2006.
- [21] T. Iqbal, B. Francois, and D. Hissel, "Dynamic modeling of a fuel cell and wind turbine DC-linked power system," in *Proc. 8th Int. Conf. Model. Simul. ELECTRIMACS*, Hammamet, Tunisia, 2004, [CD-ROM].
- [22] T. Zhou and B. Francois, "Modeling and control design of hydrogen production process for an active wind hybrid power system," *Int. J. Hydrogen Energy*, vol. 34, no. 1, pp. 21–30, Jan. 2009.
- [23] O. C. Onar, M. Uzunoglu, and M. S. Alam, "Dynamic modeling design and simulation of a wind/fuel cell/ultra-capacitor-based hybrid power generation system," *Power Sources*, vol. 161, no. 1, pp. 707–722, Oct. 2006.
- [24] J. M. Guerrero, J. Matas, G. V. Luis, M. Castilla, and J. Miret, "Decentralized control for parallel operation of distributed generation inverters using resistive output impedance," *IEEE Trans. Ind. Electron.*, vol. 54, no. 2, pp. 994–1004, Apr. 2007.
- [25] J. C. Vasquez, J. M. Guerrero, A. Luna, P. Rodriguez, and R. Teodorescu, "Adaptive droop control applied to voltage-source inverters operating in grid-connected and islanded modes," *IEEE Trans. Ind. Electron.*, vol. 56, no. 10, pp. 4048–4096, Oct. 2009.
- [26] P. Li, B. Francois, P. Degobert, and B. Robyns, "Multi-level representation for control design of a super capacitor storage system for a microgrid connected application," in *Proc. ICREPQ*, Santander, Spain, Mar. 12, 2008.
- [27] T. Zhou, P. Li, and B. François, "Power management strategies of a DC-coupled hybrid power system for microgrid operations," in *Proc. 13th Int. Eur. Power Electron. Conf. Exhib. EPE*, Barcelona, Spain, Sep. 2009, pp. 1–10, [CD-ROM].
- [28] T. Zhou and B. Francois, "Real-time emulation of a hydrogen production process for assessment of an active wind energy conversion system," *IEEE Trans. on Ind. Electron.*, vol. 56, no. 3, pp. 737–746, Mar. 2009.



Tao Zhou was born in Shandong, China, in 1981. He received the M.S. degree in power electronics and power drive from Southwest Jiaotong University, Chengdu, China, in 2006 and the Engineering degree from the Ecole Centrale de Lyon, Lyon, France, in 2006. He is currently working toward the Ph.D. degree in electrical engineering in the Laboratoire d'Electrotechnique et d'Electronique de Puissance (L2EP), Ecole Centrale de Lille, Lille, France.

His main research interests include energy management and energy storage in distributed power generation systems based on renewable energy sources.



Bruno François (M'96–SM'06) was born in Saint-Amand-les-Eaux, France, in 1969. He received the Ph.D. degree from the University of Lille, Lille, France, in 1996.

He is currently an Associate Professor with the Department of Electrical Engineering, Ecole Centrale de Lille, Lille, where he is a member of the Laboratoire d'Electrotechnique et d'Electronique de Puissance (L2EP). He is currently working on renewable-energy-based active generators and the design of advanced energy management systems.